Available online at www.sciencedirect.com
ScienceDirect
Journal of Sound and Vibration 304 (2007) 31–49
JOURNAL OF SOUND AND VIBRATION
www.elsevier.com/locate/jsvi

Wave propagation, reflection and transmission in non-uniform one-dimensional waveguides

S.-K. Lee, B.R. Mace*, M.J. Brennan

Institute of Sound and Vibration Research, University of Southampton, Highfield, Southampton SO17 1BJ, UK

Received 21 June 2005; received in revised form 14 August 2006; accepted 18 January 2007
Available online 16 April 2007

Abstract

Waves can propagate freely without reflection in a certain class of non-uniform one-dimensional waveguides even though the properties of the waveguide vary rapidly. In these cases, the amplitude of the wave changes as a function of position but the power associated with the wave is preserved along the waveguide as in uniform waveguides. A generalised wave approach based on reflection, transmission and propagation of waves is used for the analysis of such non-uniform waveguides. The positive- and negative-going wave motions are separated so that the problem is always well-posed. Examples include longitudinal motion of bars and bending motion of Euler–Bernoulli beams, where the cross-section varies as a power of the length. The energy transport velocity, which is the velocity at which energy is carried by the waves in these waveguides, is derived using the relationship between power and energy. It is shown that this energy transport velocity depends on position as well as frequency and differs from the group velocity. Numerical results for wave transmission through a rectangular connector with linearly tapered thickness and constant width are obtained in a straightforward manner without approximation errors and at a low computational cost, irrespective of frequency.

1. Introduction

The dynamic behaviour of a structure may be described in terms of waves and their propagation, reflection and transmission. This is especially suitable in the high-frequency region since it does not require powerful computing resources and is well conditioned. Of particular concern in this paper are non-uniform waveguides that have continuous variation in geometric and/or material properties.

When the degree of non-uniformity is relatively small compared to a wavelength, waves can propagate along the structure with negligible reflection as shown by Lighthill [1]. Langley [2] studied wave propagation along a slowly varying one-dimensional waveguide with deterministic, periodic and random variation using a perturbation method. He showed that the power associated with a wave component is preserved along the waveguide, while the amplitude of the wave changes as a function of position. This, however, does not happen in a general non-uniform waveguide since the energy of one wave component is transferred to another, e.g. a positive-going wave is reflected to produce a negative-going, back-scattered wave.

*Corresponding author. Tel.: +44 (0)23 8059 2344; fax: +44 (0)23 8059 3190.
E-mail address: brm@isvr.soton.ac.uk (B.R. Mace).

0022-460X/$ - see front matter © 2007 Elsevier Ltd. All rights reserved.
doi:10.1016/j.jsv.2007.01.039

Nomenclature

a	amplitude of wave
a, **b**, **c**, **d**	vectors of amplitudes of waves
A	cross-sectional area
c_l	phase velocity of longitudinal wave
c_b	phase velocity of bending wave
c^E	energy transport velocity
D	dynamic stiffness matrix for spectral element
E	modulus of elasticity
$\mathscr{E}$	energy density, $\mathscr{E} = \mathscr{T} + \mathscr{V}$
f	vector of generalised internal forces
f_{ext}	amplitude of external force
$\mathbf{f}_{\text{ext}}$	vector of amplitudes of external forces
F	propagation matrix
h	thickness
I	the second moment of area
I	identity matrix
k_l	longitudinal wavenumber
k_b	flexural wavenumber
$k_{b,m}$	effective flexural wavenumber of a section
K	external dynamic stiffness
$\mathbf{K}_{\text{ext}}$	external dynamic stiffness matrix
L	length
M	bending moment
P	longitudinal force
q	vector of amplitudes of waves induced by external forces
Q	shear force
R	reflection matrix
t	time
$\mathscr{T}$	kinetic energy density
T	transmission matrix
u	longitudinal displacement
$\mathscr{V}$	potential energy density
w	flexural displacement
w	vector of generalised displacements
x	position along waveguide axis
x_0	position where excitation is applied
α_A	taper rate for cross-sectional area, real and positive
α_I	taper rate for the second moment of area, real and positive
γ	Euler's constant, $\gamma \approx 0.577216$
θ	phase difference between two waves
μ	flaring index of a non-uniform beam, real and non-negative constant
ν	$\nu = (\mu - 1)/2$
Π	power carried by a wave
ρ	density
τ	power transmission coefficient
$\mathbf{\Phi}$	internal force matrix
$\mathbf{\Psi}$	displacement matrix
ω	angular frequency
0	null matrix

Superscripts

$+$	denote positive-going direction in x-axis
$-$	denote negative-going direction in x-axis
$\cap$	combined with **R** and **T**, denote the case where waves are incident from the right-hand side

Subscripts

0,1,2	denote position $x = x_{0,1,2}$, respectively
a	the left-hand side of a discontinuity
b	denote bending motion or the right-hand side of a discontinuity
l	denote longitudinal motion
N	denote nearfield wave

Special functions

$H_\mu^{(1,2)}$	Hankel functions of first and second kind of order μ
K_μ, I_μ	modified Bessel functions of order μ

Operators

$(\cdot)^{\mathrm{T}}$	transpose
$\mathrm{Re}(\cdot)$	real part of a quantity
$\langle \cdot \rangle$	time averaged

For non-uniform waveguides whose properties vary rapidly, wave motion can be difficult to interpret because of this reflection. However, there is a class of non-uniform waveguides, where reflection does not occur. For example, it is well-known that the governing equation of an acoustic horn can be solved for several specific shapes—the so-called Salmon's family [3]—which includes conical, exponential and catenoidal horns. Nagarkar and Finch [4] studied a bell and suggested that a sinusoidal horn could also be included in the

family. As a more general case, wave propagation in a horn where the area varies as a power of the length can be described in terms of Bessel functions [5]. The results for non-uniform acoustic waveguides can be equally applied to structural waveguides with the same variation undergoing longitudinal or torsional motion, since their governing equations all have the same mathematical form [6]. Kumma and Sujith [7] used the results to determine natural frequencies of the longitudinal vibration of some non-uniform bars.

In a class of non-uniform beams undergoing bending motion, waves can also propagate without reflection. Cranch and Adler [8] considered the case of non-uniform Euler–Bernoulli beams of rectangular cross-section. They found that when the thickness varies with position x along the beam as x, x^2 or x^3 while the width varies as an arbitrary power of x, the motion can be exactly described in terms of Bessel functions. When the cross-sectional area and moment of inertia of a non-uniform beam vary together as x^4, the equation of motion can be transformed into the wave equation [8,9]. It has also been found that the motion of non-uniform beams with exponentially varying properties can be expressed simply in terms of exponential functions [8,10]. These analytical solutions have been used to obtain natural frequencies for beams with various boundary conditions and with intermediate constraints [11–16]. Banerjee and Williams [17] used the solutions to obtain the exact dynamic stiffness matrices of some non-uniform beams. Petersson and Nijman [18] studied the dynamic characteristics of the bending wave horn, featured by a broad-banded transition from vibrations governed by the properties at the mouth to vibrations governed by those at the throat. Krylov and Tilman [19] showed that the incident flexural waves are trapped near the edge of the wedges, the thickness of which varies as a power of x, and the waves are therefore never reflected back.

The aim of this paper is to use a wave approach for the analysis of non-uniform waveguides whose properties vary rapidly but deterministically and where no wave conversion occurs. This approach facilitates physical insight into the dynamic behaviour of such waveguides, which is discussed following a description of the methodology in Section 2. Examples include longitudinal motion of non-uniform bars and bending motion of non-uniform Euler–Bernoulli beams, considered in Sections 3 and 4, respectively. For simplicity, the waveguides considered here have only geometric variation as shown in Fig. 1; the material properties are constant and damping is neglected. The response to external excitation and the spectral elements for the waveguides are derived in a systematic way. The energy transport velocity, which is the velocity at which energy is carried by the waves in these structures, is also found. Finally, numerical results are presented for the transmission of waves through a tapered connector in Section 5.

2. A generalised wave approach

In this section, a generalised approach based on reflection, transmission and propagation of waves for the analysis of one-dimensional waveguides is reviewed. The systematic formulation for the approach described here is an extension of the work of Harland et al. [20].

2.1. Representation of wave motion

Consider a one-dimensional structural waveguide lying along the x-axis. At any point, the waves can be separated into two groups according to the direction in which they travel, i.e. positive- and negative-going waves. The waves either transport energy in the corresponding direction or, if no energy flow is associated with the wave its amplitude will decay in that direction (e.g., for nearfield waves). The wave amplitudes are grouped

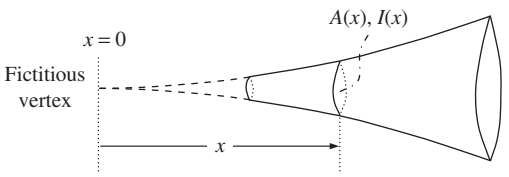

Fig. 1. Section of a non-uniform waveguide.

into two vectors $\mathbf{a}^+$ and $\mathbf{a}^-$ where the superscripts '+' and '−' denote the corresponding direction of propagation (a list of symbols is given in Nomenclature). Throughout this paper the time dependence of the motion is assumed to be of the form $e^{i\omega t}$ with angular frequency ω, but the explicit time dependence is suppressed for clarity.

In general, the motion in the waveguide is described by a partial differential equation of order $2n$. The solution gives n pairs of positive- and negative-going wave components, so that $\mathbf{a}^+$ and $\mathbf{a}^-$ are $n \times 1$ vectors.

Two illustrative examples are considered: bars undergoing longitudinal motion and Euler–Bernoulli beams undergoing bending motion. A bar is a single-mode system (i.e. $n = 1$) where only one propagating wave is associated with each direction; if the amplitudes of the two waves are given by a^+ and a^-, the wave vectors will be $\mathbf{a}^+ = \{a^+\}$ and $\mathbf{a}^- = \{a^-\}$. A beam is a two-mode system ($n = 2$) where a propagating wave and a nearfield wave are associated with each direction; now $\mathbf{a}^+ = [\,a^+ \quad a_N^+\,]^{\mathrm{T}}$ and $\mathbf{a}^- = [\,a^- \quad a_N^-\,]^{\mathrm{T}}$, where the subscript N denotes a nearfield wave.

The relationship between the state vector in the physical domain and the state vector in the wave domain is given by [20]

$$\begin{Bmatrix} \mathbf{w} \\ \mathbf{f} \end{Bmatrix} = \begin{bmatrix} \boldsymbol{\Psi}^+ & \boldsymbol{\Psi}^- \\ \boldsymbol{\Phi}^+ & \boldsymbol{\Phi}^- \end{bmatrix} \begin{Bmatrix} \mathbf{a}^+ \\ \mathbf{a}^- \end{Bmatrix}, \tag{1}$$

where $\mathbf{w}$ and $\mathbf{f}$ are $n \times 1$ vectors of generalised displacements and internal forces, respectively, and $\boldsymbol{\Psi}$ and $\boldsymbol{\Phi}$ are $n \times n$ displacement and internal force matrices describing the transformation. This transformation can always be normalised such that the elements of the first row of $\boldsymbol{\Psi}^{\pm}$ are all unity. For a *uniform* bar, where the sign convention of the physical quantities is defined as in Fig. 2(a), $\mathbf{w} = \{u\}$ and $\mathbf{f} = \{P\}$, and the displacement and internal force matrices are

$$\begin{aligned} \boldsymbol{\Psi}^+ &= [1], & \boldsymbol{\Psi}^- &= [1], \\ \boldsymbol{\Phi}^+ &= [-\mathrm{i}EAk_l], & \boldsymbol{\Phi}^- &= [\mathrm{i}EAk_l], \end{aligned} \tag{2a–d}$$

where $k_l = \sqrt{\rho\omega^2/E}$ is the longitudinal wavenumber. For a *uniform* Euler–Bernoulli beam, where the sign convention is defined as Fig. 2(b), $\mathbf{w} = [\,w \quad \partial w/\partial x\,]^{\mathrm{T}}$ and $\mathbf{f} = [\,Q \quad M\,]^{\mathrm{T}}$, and the matrices are [20]

$$\begin{aligned} \boldsymbol{\Psi}^+ &= \begin{bmatrix} 1 & 1 \\ -\mathrm{i}k_b & -k_b \end{bmatrix}, & \boldsymbol{\Psi}^- &= \begin{bmatrix} 1 & 1 \\ \mathrm{i}k_b & k_b \end{bmatrix}, \\ \boldsymbol{\Phi}^+ &= EI\begin{bmatrix} -\mathrm{i}k_b^3 & k_b^3 \\ -k_b^2 & k_b^2 \end{bmatrix}, & \boldsymbol{\Phi}^- &= EI\begin{bmatrix} \mathrm{i}k_b^3 & -k_b^3 \\ -k_b^2 & k_b^2 \end{bmatrix}, \end{aligned} \tag{3a–d}$$

where $k_b = \sqrt[4]{\rho A\omega^2/EI}$ is the flexural wavenumber. For a uniform waveguide the elements of $\boldsymbol{\Psi}$ and $\boldsymbol{\Phi}$ are invariant of x, which is not the case for a non-uniform waveguide.

Consider two points x_1 and x_2, a distance L apart, on a waveguide as shown in Fig. 3. If there is no wave mode conversion, the amplitudes of the waves at the two points are related by

$$\begin{Bmatrix} \mathbf{a}^+(x_2) \\ \mathbf{a}^-(x_1) \end{Bmatrix} = \begin{bmatrix} \mathbf{F}^+ & \mathbf{0} \\ \mathbf{0} & \mathbf{F}^- \end{bmatrix} \begin{Bmatrix} \mathbf{a}^+(x_1) \\ \mathbf{a}^-(x_2) \end{Bmatrix}, \tag{4}$$

where $\mathbf{0}$ is the null matrix, and $\mathbf{F}$ is diagonal and is termed the propagation matrix. If the waveguide is reciprocal, there is a simple relation between the positive and negative propagation matrices. Furthermore, if

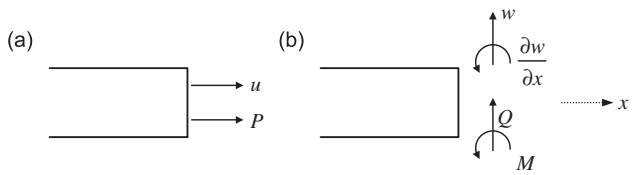

Fig. 2. Sign convention: (a) longitudinal motion, (b) bending motion.

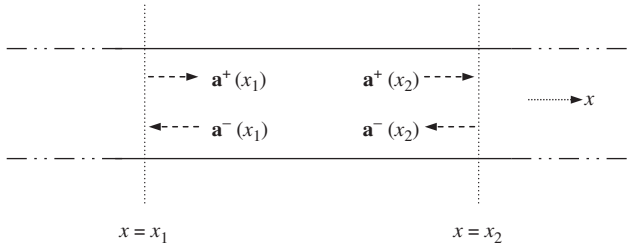

Fig. 3. Propagation of waves between two points.

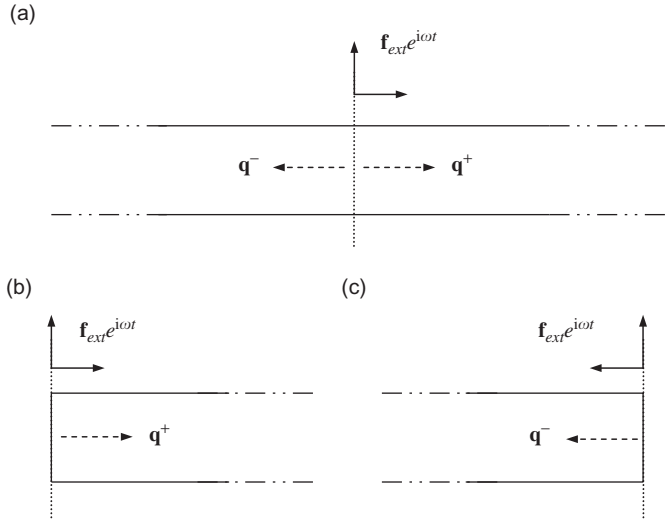

Fig. 4. A waveguide excited by local harmonic forces: (a) applied at a point, (b) applied at left-hand end, (c) applied at right-hand end.

the amplitudes of waves are normalised with respect to the power associated with the waves, then the diagonal elements of $\mathbf{F}^{\pm}$ have magnitudes, which are either constant or decrease monotonically as L increases. This arises from simple conservation of energy considerations. Thus, the analysis can be posed in a well-conditioned way. For example, the propagation matrices for a *uniform* bar and beam are, respectively, given by

$$\mathbf{F}^{\pm} = [\mathrm{e}^{-\mathrm{i}k_l L}], \quad \mathbf{F}^{\pm} = \begin{bmatrix} \mathrm{e}^{-\mathrm{i}k_b L} & 0 \\ 0 & \mathrm{e}^{-k_b L} \end{bmatrix}. \tag{5a,b}$$

For a uniform waveguide the elements depend only on the distance between the two points and the wavenumber, which is independent of position so that the positive and negative propagation matrices are the same.

2.2. Wave generation by local excitation or discontinuities

Consider a point on the waveguide excited by local harmonic forces $\mathbf{f}_{\mathrm{ext}}\mathrm{e}^{\mathrm{i}\omega t}$ as shown in Fig. 4(a). Waves of amplitudes $\mathbf{q}^+$ and $\mathbf{q}^-$ are then induced in the positive and negative directions, respectively. Applying continuity and equilibrium conditions to Eq. (1) results in

$$\mathbf{\Psi}^+\mathbf{q}^+ = \mathbf{\Psi}^-\mathbf{q}^-, \quad -\mathbf{\Phi}^+\mathbf{q}^+ + \mathbf{\Phi}^-\mathbf{q}^- = \mathbf{f}_{\mathrm{ext}}. \tag{6a,b}$$

Consequently $\mathbf{q}^+$ and $\mathbf{q}^-$ are given by

$$\mathbf{q}^+ = [-\mathbf{\Phi}^+ + \mathbf{\Phi}^-(\mathbf{\Psi}^-)^{-1}\mathbf{\Psi}^+]^{-1}\mathbf{f}_{\mathrm{ext}}, \quad \mathbf{q}^- = [\mathbf{\Phi}^- - \mathbf{\Phi}^+(\mathbf{\Psi}^+)^{-1}\mathbf{\Psi}^-]^{-1}\mathbf{f}_{\mathrm{ext}}. \tag{7a,b}$$

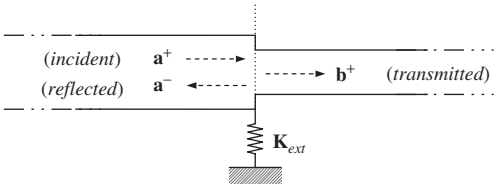

Fig. 5. Reflection and transmission of waves at a local discontinuity.

If the forces are applied at a free boundary of the waveguide as shown in Fig. 4(b,c), then waves will be induced in one direction only. The amplitudes of these waves can be obtained from Eq. (6b) by setting $\mathbf{q}^+$ or $\mathbf{q}^-$ to zero as appropriate, to give

$$\mathbf{q}^{\pm} = \mp(\mathbf{\Phi}^{\pm})^{-1}\mathbf{f}_{\text{ext}}. \tag{8a,b}$$

If there is a point discontinuity in the propagation path, waves incident on the discontinuity may be reflected and transmitted. The amplitudes of the reflected and transmitted waves are then obtained by considering the continuity and equilibrium conditions at the point. For example, consider the situation in Fig. 5, where two coaxial waveguides with different properties are joined together and there are external components, represented by the dynamic stiffness matrix $\mathbf{K}_{\text{ext}}$. The continuity and equilibrium conditions at the point are given by

$$\mathbf{w}_a = \mathbf{w}_b, \quad -\mathbf{f}_a + \mathbf{f}_b = \mathbf{K}_{\text{ext}}\mathbf{w}_a, \tag{9a,b}$$

where the subscripts a and b denote the left- and right-hand waveguides, respectively. Note that Eqs. (9a,b) do not cover all possible situations—for example, a junction between two waveguides with different numbers of wave modes [20], or a beam with a simple support. Let the amplitudes of the incident, reflected and transmitted waves, respectively, be $\mathbf{a}^+$, $\mathbf{a}^-$ and $\mathbf{b}^+$ as shown in the figure. Combining Eqs. (9a,b) with Eq. (1) gives

$$\mathbf{\Psi}_a^+\mathbf{a}^+ + \mathbf{\Psi}_a^-\mathbf{a}^- = \mathbf{\Psi}_b^+\mathbf{b}^+, \quad -\mathbf{\Phi}_a^+\mathbf{a}^+ - \mathbf{\Phi}_a^-\mathbf{a}^- + \mathbf{\Phi}_b^+\mathbf{b}^+ = \mathbf{K}_{\text{ext}}\mathbf{\Psi}_b^+\mathbf{b}^+. \tag{10a,b}$$

Thus, the amplitudes of the reflected and transmitted waves are given by

$$\mathbf{a}^- = \mathbf{R}\mathbf{a}^+, \quad \mathbf{b}^+ = \mathbf{T}\mathbf{a}^+, \tag{11a,b}$$

where $\mathbf{R}$ and $\mathbf{T}$ are reflection and transmission matrices, and are given by

$$\begin{aligned}\mathbf{R} &= -[\mathbf{K}_{\text{ext}}\mathbf{\Psi}_a^- - \mathbf{\Phi}_b^+(\mathbf{\Psi}_b^+)^{-1}\mathbf{\Psi}_a^- + \mathbf{\Phi}_a^-]^{-1}[\mathbf{K}_{\text{ext}}\mathbf{\Psi}_a^+ - \mathbf{\Phi}_b^+(\mathbf{\Psi}_b^+)^{-1}\mathbf{\Psi}_a^+ + \mathbf{\Phi}_a^+],\\ \mathbf{T} &= [\mathbf{K}_{\text{ext}}\mathbf{\Psi}_b^+ + \mathbf{\Phi}_a^-(\mathbf{\Psi}_a^-)^{-1}\mathbf{\Psi}_b^+ - \mathbf{\Phi}_b^+]^{-1}[\mathbf{\Phi}_a^-(\mathbf{\Psi}_a^-)^{-1}\mathbf{\Psi}_a^+ - \mathbf{\Phi}_a^+].\end{aligned} \tag{12a,b}$$

If the system is symmetric about the discontinuity, $\widehat{\mathbf{R}} = \mathbf{R}$ and $\widehat{\mathbf{T}} = \mathbf{T}$, where $\widehat{\cdot}$ denotes the case where waves are incident from the right-hand side of the junction. If the discontinuity represents a boundary, so that there are no transmitted waves, the reflection matrix at the boundary can be obtained from Eq. (12a) by setting the terms with the subscript b to zero.

2.3. Spectral element

A spectral element is a finite (or semi-infinite) section of a structure described by a dynamic stiffness matrix, which relates the displacements and internal forces at the ends of the element [21]. Consider again the two points x_1 and x_2 on the waveguide in Fig. 3. The displacements at these points are related to the amplitudes of the waves by

$$\mathbf{w}_1 = \mathbf{\Psi}_1^+\mathbf{a}_1^+ + \mathbf{\Psi}_1^-\mathbf{a}_1^-, \quad \mathbf{w}_2 = \mathbf{\Psi}_2^+\mathbf{a}_2^+ + \mathbf{\Psi}_2^-\mathbf{a}_2^-, \tag{13a,b}$$

where the subscripts 1 and 2 denote the positions. Since the amplitudes of the waves are related by the propagation matrices as in Eq. (4), Eqs. (13a,b) can be written as

$$\begin{Bmatrix} \mathbf{w}_1 \\ \mathbf{w}_2 \end{Bmatrix} = \begin{bmatrix} \boldsymbol{\Psi}_1^+ & \boldsymbol{\Psi}_1^- \mathbf{F}^- \\ \boldsymbol{\Psi}_2^+ \mathbf{F}^+ & \boldsymbol{\Psi}_2^- \end{bmatrix} \begin{Bmatrix} \mathbf{a}_1^+ \\ \mathbf{a}_2^- \end{Bmatrix}. \tag{14}$$

Similarly, the internal forces at the two points are given by

$$\begin{Bmatrix} \mathbf{f}_1 \\ \mathbf{f}_2 \end{Bmatrix} = \begin{bmatrix} \boldsymbol{\Phi}_1^+ & \boldsymbol{\Phi}_1^- \mathbf{F}^- \\ \boldsymbol{\Phi}_2^+ \mathbf{F}^+ & \boldsymbol{\Phi}_2^- \end{bmatrix} \begin{Bmatrix} \mathbf{a}_1^+ \\ \mathbf{a}_2^- \end{Bmatrix}. \tag{15}$$

Combining Eqs. (14) and (15) gives

$$\begin{Bmatrix} -\mathbf{f}_1 \\ \mathbf{f}_2 \end{Bmatrix} = \mathbf{D} \begin{Bmatrix} \mathbf{w}_1 \\ \mathbf{w}_2 \end{Bmatrix}, \tag{16}$$

where $\mathbf{D}$ is the dynamic stiffness matrix for the section of the waveguide and is given by

$$\mathbf{D} = \begin{bmatrix} -\boldsymbol{\Phi}_1^+ & -\boldsymbol{\Phi}_1^- \mathbf{F}^- \\ \boldsymbol{\Phi}_2^+ \mathbf{F}^+ & \boldsymbol{\Phi}_2^- \end{bmatrix} \begin{bmatrix} \boldsymbol{\Psi}_1^+ & \boldsymbol{\Psi}_1^- \mathbf{F}^- \\ \boldsymbol{\Psi}_2^+ \mathbf{F}^+ & \boldsymbol{\Psi}_2^- \end{bmatrix}^{-1}. \tag{17}$$

For a semi-infinite element (referred to as a "throw-off" element in Ref. [21]), the dynamic stiffness matrix (spectral element) is

$$\mathbf{D}^{\pm\infty} = \mp \boldsymbol{\Phi}^{\pm} (\boldsymbol{\Psi}^{\pm})^{-1}, \tag{18a,b}$$

where $\boldsymbol{\Psi}$ and $\boldsymbol{\Phi}$ are now the displacement and internal force matrices at the boundary of the semi-infinite waveguide, with the superscript denoting the appropriate direction.

3. Longitudinal waves in a non-uniform bar

In this section, the wave approach described in Section 2 is used in the analysis of the longitudinal wave motion in a *non-uniform* bar where the area varies as a power of the length. Note again that the vectors and matrices for this case consist of only one element.

3.1. Representation of wave motion

Consider the waveguide in Fig. 1 as a non-uniform bar undergoing longitudinal motion. The displacement $u(x,t)$ for free vibration is governed by [7]

$$\frac{\partial}{\partial x}\left[EA\frac{\partial u}{\partial x}\right] = \rho A \frac{\partial^2 u}{\partial t^2}. \tag{19}$$

The material properties E and ρ of the bar are assumed to be constant while the cross-sectional area A varies with x as

$$A(x) = \alpha_A x^{\mu}, \tag{20}$$

where $\alpha_A > 0$, $x > 0$ is the position from the fictitious vertex, and $\mu \geqslant 0$ is the flaring index. When $\mu = 0,1,2$, the bar could be uniform, linearly tapered in thickness, and conical, respectively. Assuming an $e^{i\omega t}$ time

dependence, substituting Eq. (20) into Eq. (19) gives

$$\frac{\mathrm{d}^2u}{\mathrm{d}x^2}+\frac{\mu}{x}\frac{\mathrm{d}u}{\mathrm{d}x}+k_l^2u=0. \tag{21}$$

The bar is undamped so that k_l is real.

Eq. (21) is a form of Bessel's equation, so the general solution can be expressed by a linear combination of Hankel functions of the first and second kinds of order $v=(\mu-1)/2$ with argument k_lx, i.e. $H_v^{(1,2)}(k_lx)$ [5]. Since the terms $H_v^{(1,2)}(k_lx)$ represent negative- and positive-going waves, respectively, the displacement is given by

$$u(x)=a^+ + a^-, \tag{22}$$

where $a^+=x^{-v}H_v^{(2)}(k_lx)C_1$ and $a^-=x^{-v}H_v^{(1)}(k_lx)C_2$, and where C_1 and C_2 are arbitrary constants. Note that the amplitudes of waves are defined such that the displacement is determined directly from the amplitudes, i.e. $a^{\pm}$ represent the amplitude of a *displacement* wave. The axial force P is then given by

$$P(x)=-EAk_l\frac{H_{v+1}^{(2)}(k_lx)}{H_v^{(2)}(k_lx)}a^+ - EAk_l\frac{H_{v+1}^{(1)}(k_lx)}{H_v^{(1)}(k_lx)}a^-. \tag{23}$$

Noting that $\mathbf{w}=\{u\}$, $\mathbf{f}=\{P\}$, $\mathbf{a}^+=\{a^+\}$ and $\mathbf{a}^-=\{a^-\}$, the displacement and internal force matrices for the non-uniform bar are given by

$$\boldsymbol{\Psi}^+=[1], \qquad \boldsymbol{\Psi}^-=[1],$$
$$\boldsymbol{\Phi}^+=\left[-EAk_l\frac{H_{v+1}^{(2)}(k_lx)}{H_v^{(2)}(k_lx)}\right], \quad \boldsymbol{\Phi}^-=\left[-EAk_l\frac{H_{v+1}^{(1)}(k_lx)}{H_v^{(1)}(k_lx)}\right]. \tag{24a–d}$$

Using the asymptotic behaviour of Bessel functions given in Appendix A, it can be shown that the internal force matrices asymptote to those for the uniform bar given by equations (2c,d) when $k_lx\gg1$ (i.e. the frequency is such that $x\gg\lambda_l/2\pi$, where λ_l is the wavelength).

The propagation matrices $\mathbf{F}^{\pm}$ between two points x and $x+L$ are given by

$$\mathbf{F}^+=\left[\left(\frac{x}{x+L}\right)^v\frac{H_v^{(2)}(k_lx+k_lL)}{H_v^{(2)}(k_lx)}\right], \quad \mathbf{F}^-=\left[\left(\frac{x+L}{x}\right)^v\frac{H_v^{(1)}(k_lx)}{H_v^{(1)}(k_lx+k_lL)}\right]. \tag{25a,b}$$

When $k_lx\gg1$, the matrices asymptote to

$$\mathbf{F}^+\approx\left(\frac{x}{x+L}\right)^{\mu/2}[\mathrm{e}^{-\mathrm{i}k_lL}] \quad \mathbf{F}^-\approx\left(\frac{x+L}{x}\right)^{\mu/2}[\mathrm{e}^{-\mathrm{i}k_lL}]. \tag{26a,b}$$

This indicates that, at high frequencies, waves in the non-uniform bar propagate as they do in the uniform bar but with their amplitudes scaled by the square root of the ratio of the characteristic impedances (defined by $A\sqrt{E\rho}$) at each end of the section.

3.2. Wave generation by local excitation

Consider a non-uniform bar with the cross-sectional area varying as Eq. (20), one end (at $x=x_0$) of which is excited by the longitudinal force $f_{\mathrm{ext}}\mathrm{e}^{\mathrm{i}\omega t}$ as shown in Fig. 4(b,c). When the left-hand end is excited (i.e. for the gradually increasing bar), the amplitude of the positive-going wave induced by the force is obtained by substituting equation (24c) into Eq. (8a) to give

$$\mathbf{q}^+=\left\{\frac{1}{EA_0k_l}\frac{H_v^{(2)}(k_lx_0)}{H_{v+1}^{(2)}(k_lx_0)}\right\}f_{\mathrm{ext}}, \tag{27}$$

where x_0 is the distance from the fictitious vertex to the end at which the force is applied and $A_0=A(x_0)$. Similarly, when the right-hand end is excited (i.e. for the gradually decreasing bar), the negative-going wave induced by the force is obtained by substituting Eq. (24d) into Eq. (8b).

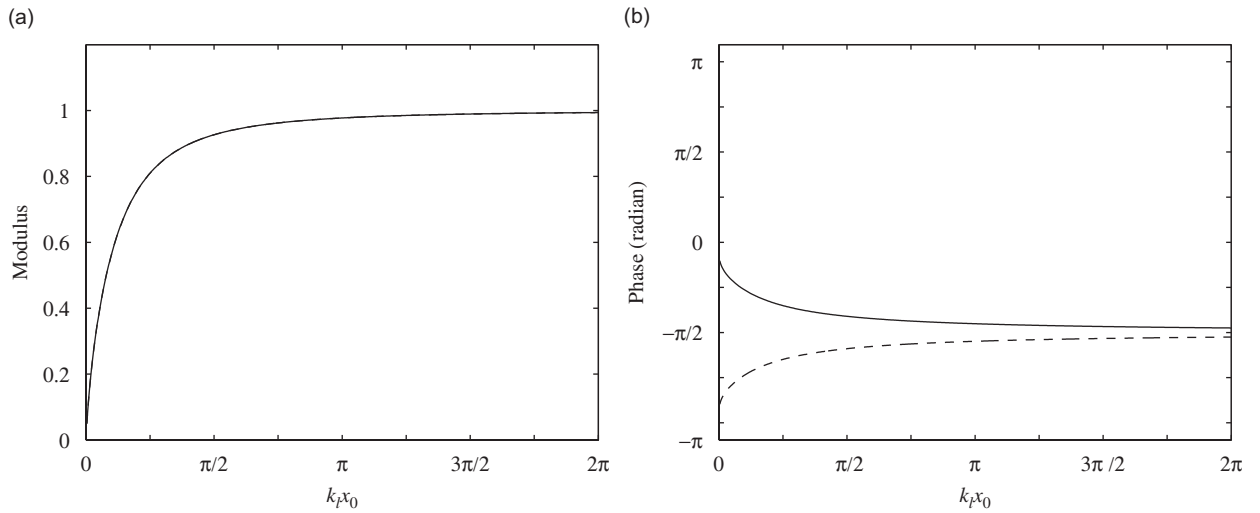

Fig. 6. Longitudinal wave generation in the non-uniform bar with $\mu = 1$ when an end is excited: (a) ratio of magnitude of induced wave to that in the uniform bar, (b) phase of induced wave; ——, left-hand end excited; ------, right-hand end excited.

When $\mu = 2$ (i.e., a "conical" bar), Eq. (27) for the gradually increasing bar simply reduces to

$$\mathbf{q}^+ = \left\{ \frac{x_0}{EA_0} \frac{1}{\mathrm{i}k_l x_0 + 1} \right\} f_{\mathrm{ext}}. \tag{28}$$

Compared to the case of the uniform bar where $\mathbf{q}^+ = f_{\mathrm{ext}}/(\mathrm{i}EA_0 k_l)$, the non-uniformity of the bar introduces a stiffness-like term EA_0/x_0 as well as the damping-like term $\mathrm{i}EA_0 k_l$. This stiffness-like term becomes dominant when $k_l x_0 \ll 1$. When $k_l x_0 \gg 1$, the stiffness-like term becomes negligible and the amplitude asymptotes to that of the uniform bar. Meanwhile, for the gradually decreasing bar, the wave amplitude is

$$\mathbf{q}^- = \left\{ \frac{x_0}{EA_0} \frac{1}{\mathrm{i}k_l x_0 - 1} \right\} f_{\mathrm{ext}}. \tag{29}$$

Now the sign of the additional term due to the non-uniformity changes so that the response shows mass-like behaviour at low frequencies.

When $\mu = 1$ (i.e. a bar whose cross-sectional area increases linearly) and $k_l x_0 \ll 1$, Eq. (27) reduces to

$$\mathbf{q}^+ \approx \left\{ -\frac{x_0}{EA_0} \left(\mathrm{i}\frac{\pi}{2} + \ln(k_l x_0) + \gamma - \ln(2) \right) \right\} f_{\mathrm{ext}}, \tag{30}$$

where $\gamma \approx 0.577\ldots$ is Euler's constant. The real part of the amplitude is positive; therefore, the response shows stiffness-dominant behaviour. Fig. 6 shows the amplitudes of the waves induced in the non-uniform bar with $\mu = 1$ when the left- and right-hand ends of the bar are excited, respectively. The magnitude is normalised by the magnitude of the wave that would be induced in the uniform bar, i.e. f_{ext}/EAk_l. The magnitudes in the two cases are equal but the phases are symmetric about $-\pi/2$. When $k_l x_0 \ll 1$, for the gradually increasing bar the phase asymptotes to zero (i.e. is stiffness-dominant) while for the gradually decreasing bar the phase asymptotes to $-\pi$ (i.e. mass-dominant).

Now consider a non-uniform bar excited at a internal point at $x = x_0$ by a longitudinal force as shown in Fig. 4(a). The amplitudes of the positive- and negative-going waves induced by the force are now identical and

$$\mathbf{q}^+ = \left\{ \frac{\pi x_0}{\mathrm{i}2EA_0} |H_\nu^{(2)}(k_l x_0)|^2 \right\} \frac{f_{\mathrm{ext}}}{2}. \tag{31}$$

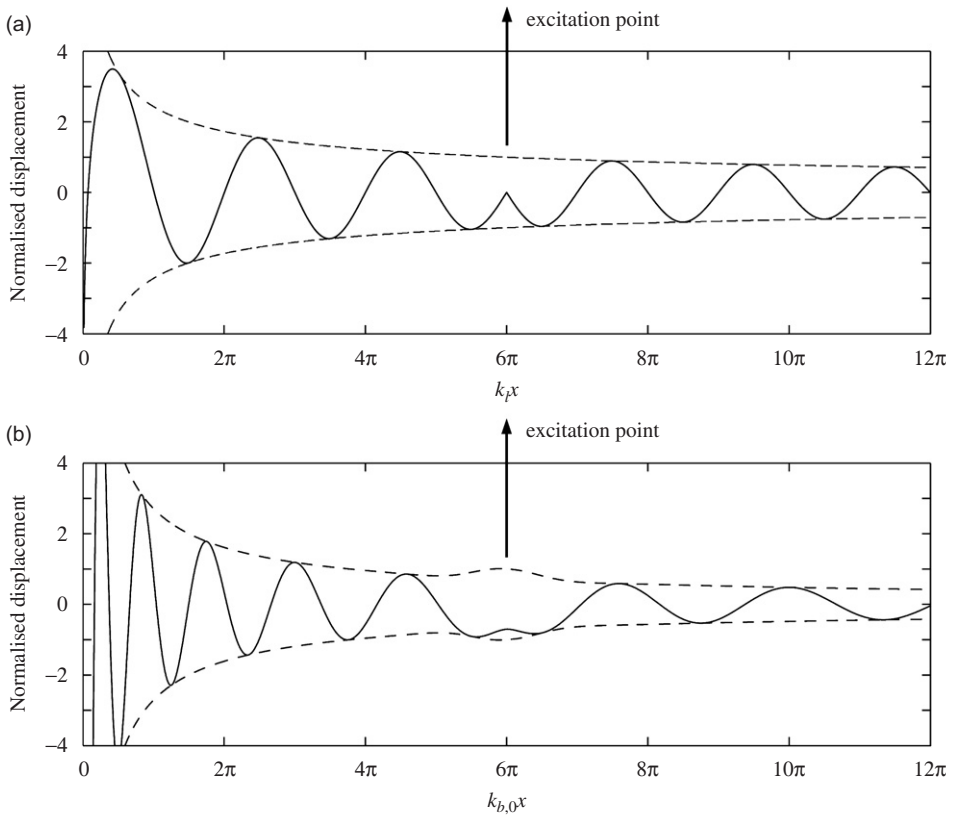

Fig. 7. (a) Response of the non-uniform bar with $\mu = 1$ due to external force: ——, displacement at time $t = 2n\pi/\omega$; ------, magnitude. (b) Response of the non-uniform beam with $\mu = 1$ due to external force: ——, displacement at time $t = 2n\pi/\omega$; ------, magnitude.

The response is purely imaginary in this case, which indicates that the reactive elements cancel each other and the response is dominated only by the damping-like term as with a uniform bar. Fig. 7(a) shows the response, normalised with respect to $f_{\text{ext}}/2EA_0k_l$, of the gradually increasing bar with $\mu = 1$ to the harmonic force. The solid line shows the displacement at time $t = 2n\pi/\omega$ for $n = 0, 1, 2 \ldots$. The dashed lines show the magnitude, which decreases as the cross-sectional area increases.

3.3. Spectral element

Following the procedure in Section 2.3 the dynamic stiffness matrix for a semi-infinite gradually increasing bar element can be determined by substituting Eqs. (24a,c) into Eq. (18a) to give

$$\mathbf{D}^{+\infty} = \left[EA_0 k_l \frac{H_{v+1}^{(2)}(k_l x_0)}{H_v^{(2)}(k_l x_0)} \right]. \tag{32}$$

Similarly, the dynamic stiffness matrix for a finite non-uniform bar can be obtained by using Eqs. (24a–d) and (25a,b) to give the dynamic stiffness matrix in Eq. (17), which is reported in Ref. [17].

3.4. Propagation of energy

For longitudinal motion of a bar the kinetic and potential energies per unit length are, respectively, given by $\mathscr{T} = 0.5\rho A\{\text{Re}(\partial u/\partial t)\}^2$ and $\mathscr{V} = 0.5EA\{\text{Re}(\partial u/\partial x)\}^2$ [22], where $\text{Re}(\cdot)$ denotes the real part. If there is only a positive-going wave with amplitude a^+, the displacement will be $u(x) = a^+$ thus the time-averaged energy

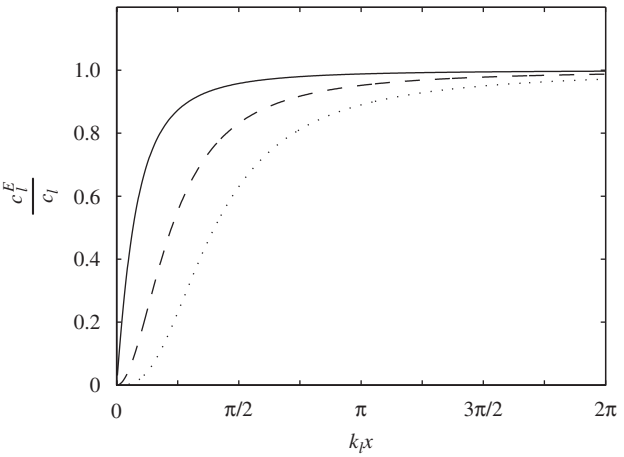

Fig. 8. Ratio of energy transport velocity of longitudinal wave to the phase velocity: ——, $\mu = 1$; ------, $\mu = 2$; ……, $\mu = 3$.

densities associated with the wave are given by

$$\langle \mathscr{T} \rangle = \frac{1}{4}\rho A\omega^2 |a^+|^2, \quad \langle \mathscr{V} \rangle = \frac{1}{4}\rho A\omega^2 |a^+|^2 \left| \frac{H_{v+1}^{(2)}(k_l x)}{H_v^{(2)}(k_l x)} \right|^2, \tag{33a,b}$$

where $\langle \cdot \rangle$ indicates a time-averaged quantity. Note that, when $\mu = 0$ (i.e., a uniform bar), the kinetic and potential energy densities are the same but, for the other cases, $\langle \mathscr{V} \rangle > \langle \mathscr{T} \rangle$ in the region of $k_l x < \pi$. As $k_l x$ increases, the energy densities become the same. The total energy density is given by

$$\langle \mathscr{E} \rangle = \langle \mathscr{T} \rangle + \langle \mathscr{V} \rangle = \frac{1}{4}\rho A\omega^2 |a^+|^2 \frac{|H_v^{(2)}(k_l x)|^2 + |H_{v+1}^{(2)}(k_l x)|^2}{|H_v^{(2)}(k_l x)|^2}. \tag{34}$$

The time-averaged power for longitudinal motion of a bar is given by $\langle \Pi \rangle = -\langle \mathrm{Re}(P) \cdot \mathrm{Re}(\partial u/\partial t) \rangle$ [22]; therefore, the power associated with the positive-going wave is

$$\langle \Pi \rangle = \rho A\omega^2 |a^+|^2 \frac{c_l}{\pi k_l x} |H_v^{(2)}(k_l x)|^{-2}, \tag{35}$$

where $c_l = \omega/k_l$ is the phase velocity of the longitudinal wave. Noting that $a^+ = x^{-v} H_v^{(2)}(k_l x) C_1$, it follows that the power is constant along the bar. This is of course obvious from conservation of energy considerations. In terms of the total energy density and the power, the energy transport velocity is given as $c^E = \langle \Pi \rangle / \langle \mathscr{E} \rangle$ [1], thus

$$c_l^E = \frac{4c_l}{\pi k_l x} (|H_v^{(2)}(k_l x)|^2 + |H_{v+1}^{(2)}(k_l x)|^2)^{-1}. \tag{36}$$

Specifically, when $\mu = 2$, Eq. (36) reduces to

$$c_l^E = \frac{c_l}{1 + (\sqrt{2} k_l x)^{-2}}. \tag{37}$$

The energy transport velocity is generally different to the group velocity, which is formally defined by $c_g = \mathrm{d}\omega/\mathrm{d}k$ (for real wavenumbers). Note that, for a non-uniform bar, $c_g = c_l$. The energy transport velocity associated with the negative-going wave is the same as that associated with the positive-going wave as would be expected from physical considerations. Fig. 8 shows the energy transport velocity, normalised with respect to the longitudinal velocity c_l, for a non-uniform bar with three different values of μ. It can be seen that the velocity decreases as μ increases, i.e. as the degree of non-uniformity increases. When $k_l x \ll 1$, the velocity is approximately proportional to $(k_l x)^\mu$. The velocity increases as $k_l x$ increases and finally asymptotes to that of a uniform bar.

4. Bending waves in a non-uniform beam

In this section, the wave approach is applied to bending motion of a *non-uniform* Euler–Bernoulli beam for which the cross-sectional area and the second moment of area vary as $A(x) \propto x^{\mu}$ and $I(x) \propto x^{\mu+2}$, respectively. The development is similar to that described for a non-uniform bar in the previous section. However, the displacement, internal force and propagation matrices for the non-uniform beam are of order 2×2.

4.1. Representation of wave motion

Consider the waveguide shown in Fig. 1 as a non-uniform Euler–Bernoulli beam undergoing bending motion. The lateral displacement $w(x,t)$ for free vibration is governed by [8]

$$\frac{\partial^2}{\partial x^2}\left[EI\frac{\partial^2 w}{\partial x^2}\right] + \rho A\frac{\partial^2 w}{\partial t^2} = 0. \tag{38}$$

The material properties of the beam are assumed to be constant while the cross-sectional area A and the second moment of area I vary as

$$A(x) = \alpha_A x^{\mu}, \quad I(x) = \alpha_I x^{\mu+2}, \tag{39a,b}$$

where α_I is positive. When $\mu = 1$ and the cross-section is rectangular, the beam has linearly varying thickness and constant width. Substituting Eqs. (39a,b) into Eq. (38) and assuming an $e^{i\omega t}$ time dependence gives

$$x^2\frac{d^4 w}{dx^4} + 2(\mu+2)x\frac{d^3 w}{dx^3} + (\mu+1)(\mu+2)\frac{d^2 w}{dx^2} - k_b^4 x^2 w = 0, \tag{40}$$

where $k_b(x) = \sqrt[4]{\rho A(x)\omega^2/EI(x)}$. It can be noted that k_b is proportional to $\sqrt{\omega/x}$ in this case. Hereafter, if there is no specific indication, k_b means the wavenumber $k_b(x)$ at position x.

Eq. (40) can be factorised into the product of the Bessel equation and the modified Bessel equation [8] so that the general solution can be expressed by a linear combination of Hankel functions of order μ with argument $2k_b x$, $H_{\mu}^{(1,2)}(2k_b x)$, and modified Bessel functions, $Y_{\mu}(2k_b x)$ and $I_{\mu}(2k_b x)$. The terms $H_{\mu}^{(1,2)}$ represent negative- and positive-going propagating waves, respectively, and the terms K_{μ} and I_{μ} the positive- and negative-going nearfield waves, respectively. Thus the solution of Eq. (40) is given by

$$w(x) = a^{+} + a_N^{+} + a^{-} + a_N^{-}, \tag{41}$$

where a^{+}, a_{N}^{+}, a^{-} and a_{N}^{-} are the amplitudes of the four waves at position x. They are given by

$$\begin{aligned} a^{+} &= x^{-\mu/2}H_{\mu}^{(2)}(2k_b x)C_1, \quad a_N^{+} = x^{-\mu/2}K_{\mu}(2k_b x)C_2, \\ a^{-} &= x^{-\mu/2}H_{\mu}^{(1)}(2k_b x)C_3, \quad a_N^{-} = x^{-\mu/2}I_{\mu}(2k_b x)C_4, \end{aligned} \tag{42a–d}$$

where $C_{1,2,3,4}$ are arbitrary constants. The shear force and bending moment can also be expressed in terms of the amplitudes of the waves in a straightforward manner.

Noting that $\mathbf{w} = [\,w \quad dw/dx\,]^{\mathrm{T}}$, $\mathbf{f} = [\,Q \quad M\,]^{\mathrm{T}}$, $\mathbf{a}^{+} = [\,a^{+} \quad a_N^{+}\,]^{\mathrm{T}}$ and $\mathbf{a}^{-} = [\,a^{-} \quad a_N^{-}\,]^{\mathrm{T}}$, the displacement and internal force matrices for the non-uniform beam are given by

$$\boldsymbol{\Psi}^{+} = \begin{bmatrix} 1 & 1 \\ -k_b\dfrac{H_{\mu+1}^{(2)}(2k_b x)}{H_{\mu}^{(2)}(2k_b x)} & -k_b\dfrac{K_{\mu+1}(2k_b x)}{K_{\mu}(2k_b x)} \end{bmatrix}, \quad \boldsymbol{\Psi}^{-} = \begin{bmatrix} 1 & 1 \\ -k_b\dfrac{H_{\mu+1}^{(1)}(2k_b x)}{H_{\mu}^{(1)}(2k_b x)} & k_b\dfrac{I_{\mu+1}(2k_b x)}{I_{\mu}(2k_b x)} \end{bmatrix},$$

$$\boldsymbol{\Phi}^{+} = EI\begin{bmatrix} -k_b^3\dfrac{H_{\mu+1}^{(2)}(2k_b x)}{H_{\mu}^{(2)}(2k_b x)} & k_b^3\dfrac{K_{\mu+1}(2k_b x)}{K_{\mu}(2k_b x)} \\ k_b^2\dfrac{H_{\mu+2}^{(2)}(2k_b x)}{H_{\mu}^{(2)}(2k_b x)} & k_b^2\dfrac{K_{\mu+2}(2k_b x)}{K_{\mu}(2k_b x)} \end{bmatrix}, \quad \boldsymbol{\Phi}^{-} = EI\begin{bmatrix} -k_b^3\dfrac{H_{\mu+1}^{(1)}(2k_b x)}{H_{\mu}^{(1)}(2k_b x)} & -k_b^3\dfrac{I_{\mu+1}(2k_b x)}{I_{\mu}(2k_b x)} \\ k_b^2\dfrac{H_{\mu+2}^{(1)}(2k_b x)}{H_{\mu}^{(1)}(2k_b x)} & k_b^2\dfrac{I_{\mu+2}(2k_b x)}{I_{\mu}(2k_b x)} \end{bmatrix}. \tag{43a–d}$$

When $2k_b x \gg 1$, the matrices for the non-uniform beam asymptote to those for the uniform beam given by Eqs. (3a–d).

Using the expressions for the wave amplitudes together with Eq. (4) the propagation matrices $\mathbf{F}^{\pm}$ between two points x and $x+L$ are found to be

$$\mathbf{F}^{+} = \left(\frac{x}{x+L}\right)^{\mu/2} \begin{bmatrix} \dfrac{H_\mu^{(2)}\left(2k_b\sqrt{x(x+L)}\right)}{H_\mu^{(2)}(2k_b x)} & 0 \\ 0 & \dfrac{K_\mu\left(2k_b\sqrt{x(x+L)}\right)}{K_\mu(2k_b x)} \end{bmatrix},$$

$$\mathbf{F}^{-} = \left(\frac{x+L}{x}\right)^{\mu/2} \begin{bmatrix} \dfrac{H_\mu^{(1)}(2k_b x)}{H_\mu^{(1)}\left(2k_b\sqrt{x(x+L)}\right)} & 0 \\ 0 & \dfrac{I_\mu(2k_b x)}{I_\mu\left(2k_b\sqrt{x(x+L)}\right)} \end{bmatrix}. \tag{44a, b}$$

When $2k_b x \gg 1$, the positive- and negative-going propagation matrices asymptote to

$$\mathbf{F}^{+} \approx \left(\frac{x}{x+L}\right)^{((\mu/2)/(1/4))} \begin{bmatrix} \mathrm{e}^{-\mathrm{i}k_{b,m}L} & 0 \\ 0 & \mathrm{e}^{-k_{b,m}L} \end{bmatrix},$$

$$\mathbf{F}^{-} \approx \left(\frac{x+L}{x}\right)^{((\mu/2)/(1/4))} \begin{bmatrix} \mathrm{e}^{-\mathrm{i}k_{b,m}L} & 0 \\ 0 & \mathrm{e}^{-k_{b,m}L} \end{bmatrix}, \tag{45a, b}$$

where $k_{b,m}$ is given by

$$\frac{1}{k_{b,m}} = \frac{1}{2}\left(\frac{1}{k_b(x)} + \frac{1}{k_b(x+L)}\right). \tag{46}$$

The wavenumber $k_{b,m}$ is the *effective* flexural wavenumber in the section between the two points. Thus, the *effective* wavelength is simply the average of the wavelengths at each end of the section. Eqs. (45a,b) indicate that, for high wavenumbers or when the position is far away from the fictitious vertex, waves propagate as if in a uniform beam. However, they have an effective wavenumber given by Eq. (46) and their amplitudes are scaled by the square root of the ratio of the characteristic impedances (defined by $2EIk_b^3/\omega$) at each end of the section.

4.2. Wave generation by local excitation

Consider a non-uniform beam with geometric variation satisfying Eq. (39), one end (at $x = x_0$) of which is excited by the lateral force $f_{\mathrm{ext}}\mathrm{e}^{\mathrm{i}\omega t}$ as shown in Fig. 4(b,c). When the left-hand end is excited (i.e. for the gradually increasing beam), the amplitudes of the induced positive-going waves are found by substituting Eq. (43c) into Eq. (8a). The external force vector in this case is $\mathbf{f}_{\mathrm{ext}} = [f_{\mathrm{ext}} \quad 0]^{\mathrm{T}}$; therefore,

$$\mathbf{q}^{+} = \frac{k_b^2}{\mathrm{Det}(\mathbf{\Phi}^{+})} \begin{Bmatrix} -\dfrac{K_{\mu+2}(2k_b x)}{K_\mu(2k_b x)} \\ \dfrac{H_{\mu+2}^{(2)}(2k_b x)}{H_\mu^{(2)}(2k_b x)} \end{Bmatrix} f_{\mathrm{ext}}, \tag{47}$$

where x_0 is the distance from the fictitious vertex to the end, $k_{b,0} = k_b(x_0)$, $I_0 = I(x_0)$, and

$$\mathrm{Det}(\mathbf{\Phi}^{+}) = -EI_0 k_{b,0}^5 \frac{H_{\mu+1}^{(2)}(2k_{b,0}x_0)K_{\mu+2}(2k_{b,0}x_0) + H_{\mu+2}^{(2)}(2k_{b,0}x_0)K_{\mu+1}(2k_{b,0}x_0)}{H_\mu^{(2)}(2k_{b,0}x_0)K_\mu(2k_{b,0}x_0)}.$$

When $\mu = 1$ and $2k_{b,0}x_0 \ll 1$, using the asymptotic behaviour of Bessel functions given in Appendix A, it can be shown that Eq. (47) asymptotes to

$$\mathbf{q}^+ \approx \frac{x_0}{EI_0 k_{b,0}^2} \left\{ \begin{array}{c} 1 \\ -1 \end{array} \right\} \frac{f_{\text{ext}}}{2}. \tag{48}$$

Eq. (48) indicates that the propagating and nearfield components represent frequency dependent stiffness- and mass-like responses, respectively, with equal magnitude. The displacement asymptotes to

$$w \approx -\frac{x_0^3}{EI_0} \left\{ \mathrm{i}\frac{\pi}{2} + 2\left(\ln(k_{b,0}x_0) + \gamma - \frac{1}{4} \right) \right\} f_{\text{ext}}, \tag{49}$$

which is consistent with the point mobility given in Ref. [18].

If the right-hand end of the beam is excited (i.e. for the gradually decreasing beam), the amplitudes of the negative-going waves induced by the force are obtained by substituting Eq. (43d) into Eq. (8b). When $\mu = 1$

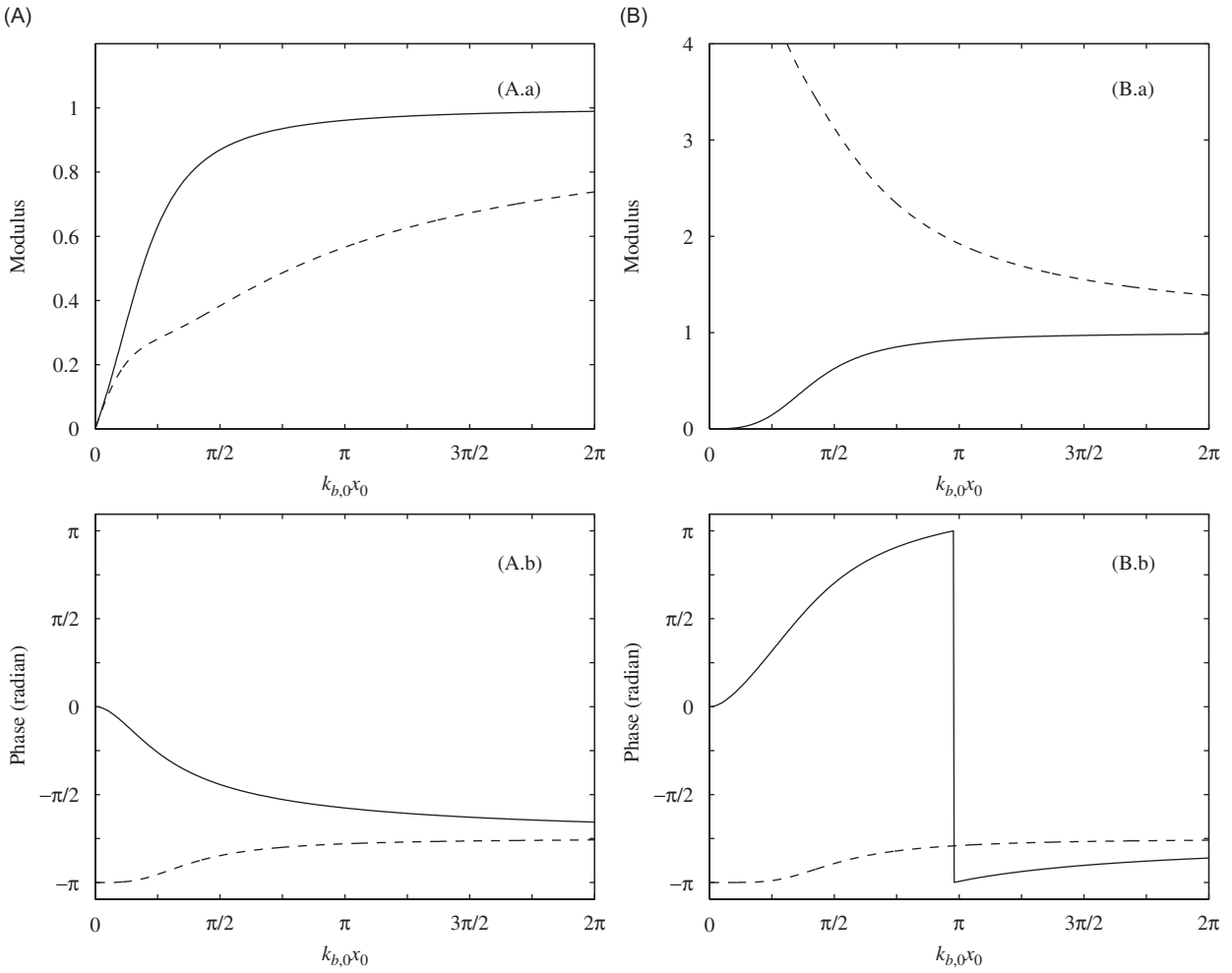

Fig. 9. Bending wave generation in the non-uniform beam with $\mu = 1$ when (A) the left- or (B) the right-hand end is excited: (a) ratio of magnitude of induced wave to that in the uniform beam, (b) phase of induced wave; ——, propagating component; ------, nearfield component.

and $2k_{b,0}x_0 \ll 1$,

$$\mathbf{q}^- \approx \frac{1}{EI_0k_{b,0}^3}\begin{Bmatrix}(k_{b,0}x_0)^3/6\\ -2/(k_{b,0}x_0)\end{Bmatrix}f_{\text{ext}}. \tag{50}$$

It can be seen that the propagating component is negligible compared to the nearfield component and the response exhibits rigid body motion with a mass equal to $\rho A_0x_0/2$.

Fig. 9A and B, respectively, show the waves induced in the non-uniform beam with $\mu = 1$ when the left- and right-hand end of the beam are excited by a lateral force. In the figure, the magnitude is normalised by $f_{\text{ext}}/\sqrt{2}EI_0k_{b,0}^3$, and $k_{b,0}x_0$ for the horizontal axis is proportional to $\sqrt{\omega x_0}$. When the right-hand end is excited, it is seen that the magnitude of the nearfield wave becomes large when $2k_{b,0}x_0 \ll 1$. Such limiting behaviour is consistent with the discussion above.

Now consider a non-uniform beam excited at an internal point $x = x_0$ by a lateral force as shown in Fig. 4(a). The amplitudes of the positive- and negative-going waves induced by the force are now identical and

$$\mathbf{q}^+ = -\frac{x_0}{EI_0k_{b,0}^2}\begin{Bmatrix}\mathrm{i}\pi|H_\mu^{(2)}(2k_{b,0}x_0)|^2\\ 4K_\mu(2k_{b,0}x_0)I_\mu(2k_{b,0}x_0)\end{Bmatrix}\frac{f_{\text{ext}}}{4}. \tag{51}$$

The propagating component is now purely imaginary representing damping-like behaviour while the nearfield component is negative-real representing mass-like behaviour. Fig. 7(b) shows the response, normalised with respect to $\sqrt{2}f_{\text{ext}}/4EI_0k_{b,0}^3$, of the gradually increasing beam with $\mu = 1$ to the harmonic force. The solid line shows the displacement at time $t = 2n\pi/\omega$ for $n = 0, 1, 2\ldots$ and the dashed lines show the magnitude. Compared to Fig. 7(a), the dependence of the phase change on the position can easily be noticed. The nearfield effect around the excitation point can also be seen.

4.3. Spectral element

Substituting Eqs. (43a,c) into Eq. (18a) gives the dynamic stiffness matrix at the boundary for the semi-infinite gradually increasing beam such that

$$\mathbf{D}^{+\infty} = \frac{EI_0}{\Delta}\begin{bmatrix}\hat{D}_{11} & \hat{D}_{12}\\ \hat{D}_{21} & \hat{D}_{22}\end{bmatrix}, \tag{52}$$

where

$$\begin{aligned}
\Delta &= H_{\mu+1}^{(2)}(2k_{b,0}x_0)K_\mu(2k_{b,0}x_0) - K_{\mu+1}(2k_{b,0}x_0)H_\mu^{(2)}(2k_{b,0}x_0),\\
\hat{D}_{11} &= -2k_{b,0}^3H_{\mu+1}^{(2)}(2k_{b,0}x_0)K_{\mu+1}(2k_{b,0}x_0),\\
\hat{D}_{12} &= \hat{D}_{21} = -k_{b,0}^2\{H_{\mu+1}^{(2)}(2k_{b,0}x_0)K_\mu(2k_{b,0}x_0) + K_{\mu+1}(2k_{b,0}x_0)H_\mu^{(2)}(2k_{b,0}x_0)\},\\
\hat{D}_{22} &= k_{b,0}\{H_{\mu+2}^{(2)}(2k_{b,0}x_0)K_\mu(2k_{b,0}x_0) - K_{\mu+2}(2k_{b,0}x_0)H_\mu^{(2)}(2k_{b,0}x_0)\}.
\end{aligned} \tag{53a–d}$$

When $2k_{b,0}x_0 \gg 1$, the matrix asymptotes to that of the semi-infinite uniform beam, i.e.

$$\mathbf{D} \approx EI_0\begin{bmatrix}-(1-\mathrm{i})k_{b,0}^3 & \mathrm{i}k_{b,0}^2\\ \mathrm{i}k_{b,0}^2 & (1+i)k_{b,0}\end{bmatrix}. \tag{54}$$

The dynamic stiffness matrix for the finite non-uniform beam can be also obtained in a similar way to that described for the uniform bar to give the result in Ref. [17].

4.4. Propagation of energy

The kinetic and potential energy densities for bending motion of a beam are, respectively, given by $\mathscr{T} = 0.5\rho A\{\mathrm{Re}(\partial w/\partial t)\}^2$ and $\mathscr{V} = 0.5EI\{\mathrm{Re}(\partial^2 w/\partial x^2)\}^2$ [22]. If there is only the propagating component of the positive-going waves in the non-uniform beam, i.e. $\mathbf{a}^+ = [a^+ \quad 0]^{\mathrm{T}}$, the displacement of the beam will be

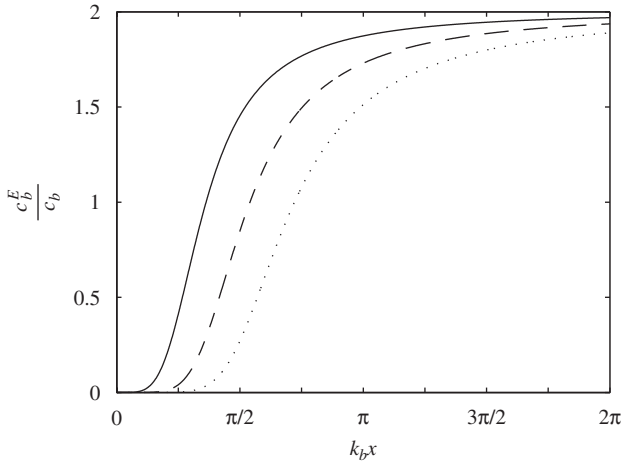

Fig. 10. Ratio of energy transport velocity of a bending wave of a non-uniform beam to the phase velocity: ——, $\mu = 1$; ------, $\mu = 2$; ……, $\mu = 3$.

$w(x) = a^+$. For time harmonic motion, the time-averaged energy densities associated with this component are

$$\langle \mathscr{T} \rangle = \frac{1}{4}\rho A\omega^2 |a^+|^2, \quad \langle \mathscr{V} \rangle = \frac{1}{4}\rho A\omega^2 |a^+|^2 \frac{|H_{\mu+2}^{(2)}(2k_b x)|^2}{|H_{\mu}^{(2)}(2k_b x)|^2}. \tag{55a,b}$$

Note that $\langle \mathscr{V} \rangle > \langle \mathscr{T} \rangle$, especially, in the region of $k_l x < \pi$. As $k_l x$ increases, the energy densities become the same. The total energy density is then

$$\langle \mathscr{E} \rangle = \frac{1}{4}\rho A\omega^2 |a^+|^2 \frac{|H_{\mu}^{(2)}(2k_b x)|^2 + |H_{\mu+2}^{(2)}(2k_b x)|^2}{|H_{\mu}^{(2)}(2k_b x)|^2}. \tag{56}$$

The time-averaged power for bending motion of a beam is given by $\langle \Pi \rangle = -\langle \mathrm{Re}(Q) \cdot \mathrm{Re}(\partial w/\partial t) + \mathrm{Re}(M) \cdot \mathrm{Re}(\partial/\partial t(\partial w/\partial x)) \rangle$ [22]. Thus, the energy flow associated with the propagating wave component is

$$\langle \Pi \rangle = \rho A\omega^2 |a^+|^2 \frac{c_b}{\pi k_b x} |H_{\mu}^{(2)}(2k_b x)|^{-2}, \tag{57}$$

where c_b is the phase velocity of the bending wave at x. Noting that a^+ is given by Eq. (42a), it follows again that the power is constant along the beam. Finally, the energy transport velocity for the bending wave is found by combining Eqs. (56) and (57) with $c^E = \langle \Pi \rangle / \langle \mathscr{E} \rangle$ to give

$$c_b^E = \frac{4c_b}{\pi k_b x} (|H_{\mu}^{(2)}(2k_b x)|^2 + |H_{\mu+2}^{(2)}(2k_b x)|^2)^{-1}. \tag{58}$$

The energy transport velocity associated with the propagating positive-going wave component is the same as that associated with the negative-going wave component.

Fig. 10 shows the energy transport velocity, normalised with respect to c_b, for the non-uniform beam with three different values of μ. The behaviour is similar to that of the longitudinal wave described in Section 3.4. When $2k_b x \ll 1$, the velocity is approximately proportional to $(k_b x)^{2\mu+4}$. When $2k_b x \gg 1$, the velocity asymptotes to the group velocity of the uniform beam, i.e. $c_b^E = 2c_b$.

5. Numerical example

In this section, the propagation of waves through a rectangular non-uniform waveguide of length L sandwiched between two semi-infinite uniform rectangular waveguides as shown in Fig. 11 is considered. The non-uniform element has constant width but tapered thickness and the semi-infinite waveguides have the same width but thicknesses, h_1 and h_2. Numerical results are presented for the transmission of longitudinal and bending waves through the tapered waveguide using the results of Sections 3 and 4. For simplicity, the

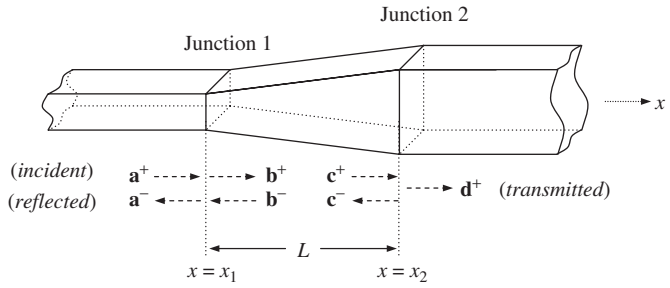

Fig. 11. A rectangular connector tapered in thickness.

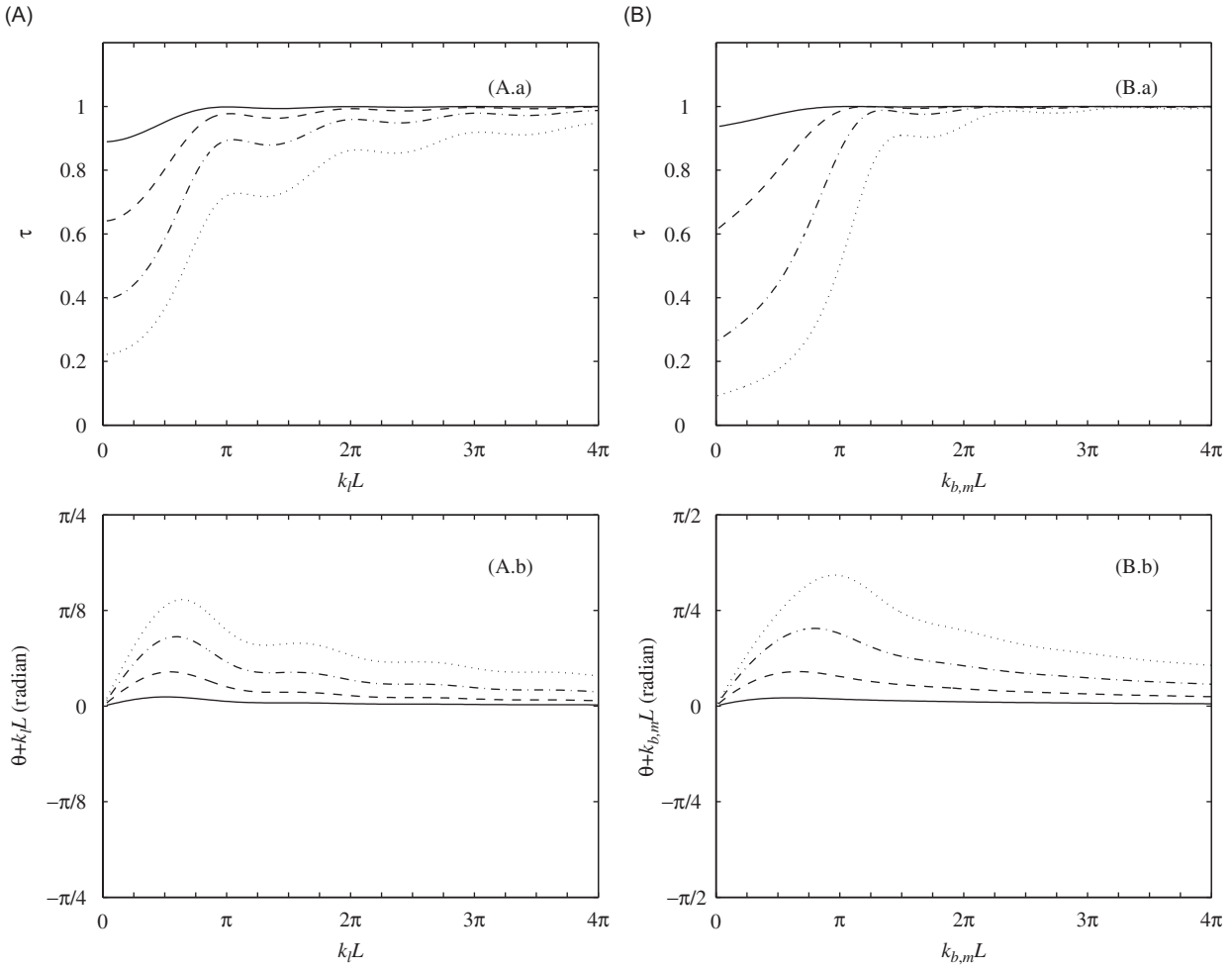

Fig. 12. Transmission of the propagating component of (A) longitudinal and (B) bending wave through the connector: (a) power transmission coefficient τ, (b) phase difference θ between incident and transmitted propagating wave components, plus the mean phase change in the connector; ——, $h_2/h_1 = 2$; - - - - - -, $h_2/h_1 = 4$; - · - · - · - · -, $h_2/h_1 = 8$; ……, $h_2/h_1 = 16$.

material properties of the connector and the waveguides are assumed to all be the same. The thickness of the connector varies with x as

$$h(x) = h_1 x/x_1, \tag{59}$$

where $x \geqslant x_1$ and $x_1 = h_1 L/(h_2 - h_1)$ is the position from the vertex to junction 1.

Consider waves $\mathbf{a}^+$ incident on the connector from the left-hand uniform waveguide. As shown in Fig. 11 the waves at the junctions are denoted by $\mathbf{b}^{\pm}$, $\mathbf{c}^{\pm}$ and $\mathbf{d}^+$; the relationships between the waves are

$$\mathbf{b}^+ = \mathbf{T}_1\mathbf{a}^+ + \widehat{\mathbf{R}}_1\mathbf{b}^-, \quad \mathbf{c}^+ = \mathbf{F}^+\mathbf{b}^+, \quad \mathbf{c}^- = \mathbf{R}_2\mathbf{c}^+, \quad \mathbf{b}^- = \mathbf{F}^-\mathbf{c}^-, \quad \mathbf{a}^- = \mathbf{R}_1\mathbf{a}^+ + \widehat{\mathbf{T}}_1\mathbf{b}^-, \quad \mathbf{d}^+ = \mathbf{T}_2\mathbf{c}^+, \qquad (60a-f)$$

where $\mathbf{R}_1$, $\mathbf{T}$, etc., are the reflection and transmission matrices at the junctions, and $\mathbf{F}^+$ and $\mathbf{F}^-$ are the propagation matrices between the junctions. These matrices can be obtained from the results of the previous sections. Rearranging Eq. (60) in terms of the incident waves $\mathbf{a}^+$ yields [23]

$$\mathbf{a}^- = [\mathbf{R}_1 + \widehat{\mathbf{T}}_1\mathbf{F}^-\mathbf{R}_2\mathbf{F}^+[\mathbf{I} - \widehat{\mathbf{R}}_1\mathbf{F}^-\mathbf{R}_2\mathbf{F}^+]^{-1}\mathbf{T}_1]\mathbf{a}^+,$$

$$\mathbf{d}^+ = [\mathbf{T}_2\mathbf{F}^+[\mathbf{I} - \widehat{\mathbf{R}}_1\mathbf{F}^-\mathbf{R}_2\mathbf{F}^+]^{-1}\mathbf{T}_1]\mathbf{a}^+, \qquad (61a, b)$$

where $\mathbf{I}$ is the identity matrix. The reflected waves $\mathbf{a}^-$ have components from the direct reflection of the incident waves ($\mathbf{R}_1\mathbf{a}^+$), while the remaining components arise from waves which are initially transmitted through the junction 1 and are then subsequently reflected back-and-forth at the two junctions. The net reflected waves are thus the superposition of the direct and subsequent reflected components. Similarly, the transmitted waves $\mathbf{d}^+$ consist of the direct components transmitted through the two junctions ($\mathbf{T}_2\mathbf{F}^+\mathbf{T}_1\mathbf{a}^+$), and the components from the subsequent reflections between the two junctions.

Suppose that a propagating wave component of amplitude $\mathbf{a}^+$ is incident on the connector, i.e. $\mathbf{a}^+ = \{a^+\}$ for longitudinal motion and $\mathbf{a}^+ = [a^+ \quad 0]^{\mathrm{T}}$ for bending motion. Fig. 12 shows numerical results for the transmission through the connector. When $kL \gg 1$ (k_l for the longitudinal and $k_{b,m}$ given by Eq. (46) for the bending, respectively), the power transmission coefficient $\tau \to 1$, i.e. the power incident on the connector is totally transmitted when frequency increases or the non-uniformity decreases. The phase difference θ between the incident and transmitted propagating components then asymptotes to $-kL$. When $kL \ll 1$, the results asymptote to those of the case where the two uniform waveguides are directly connected without the connector [22].

6. Concluding remarks

A wave approach based on reflection, transmission and propagation of waves has been used for the analysis of non-uniform waveguides, where the properties vary rapidly but where no wave mode conversion occurs. It was demonstrated for longitudinal motion of bars and bending motion of Euler–Bernoulli beams, where the cross-section varies as a power of the length. The state vector in the physical domain was transformed to the wave domain using the displacement and internal force matrices. The wave amplitudes at one point were related to those at another point by the diagonal propagation matrix. Since the positive- and negative-going wave motions are separately considered in the approach, the problem is always well-posed even when nearfield waves exist.

The response to external excitation and the spectral element for the waveguides were obtained in a systematic way. The energy transport velocity, which is the velocity at which energy is carried by the waves in these waveguides, was also derived using the relationship between power and energy. It was shown that this energy transport velocity depends on position as well as frequency and differs from the group velocity. Finally, numerical results for wave transmission through the tapered connector were obtained in a straightforward manner without approximation errors and at a low computational cost, irrespective of frequency.

Appendix A. Asymptotic behaviour of Bessel functions

For large argument $|z| \gg 1$ and $-\pi < \arg(z) < 2\pi$, the Hankel functions of order v asymptote to [24]

$$H_v^{(1)}(z) \approx \sqrt{\frac{2}{\pi z}}\mathrm{e}^{\mathrm{i}(z-\frac{1}{4}\pi-\frac{1}{2}v\pi)}, \quad H_v^{(2)}(z) \approx \sqrt{\frac{2}{\pi z}}\mathrm{e}^{-\mathrm{i}(z-\frac{1}{4}\pi-\frac{1}{2}v\pi)}. \qquad (A.1a,b)$$

Thus, it follows that

$$\frac{H_{v+1}^{(1)}(z)}{H_v^{(1)}(z)} \approx -i, \quad \frac{H_{v+1}^{(2)}(z)}{H_v^{(2)}(z)} \approx i, \quad \frac{H_{v+2}^{(1)}(z)}{H_v^{(1)}(z)} \approx -1, \quad \frac{H_{v+2}^{(2)}(z)}{H_v^{(2)}(z)} \approx -1. \qquad (A.2a-d)$$

When z is real, the modified Bessel functions $K_v(z)$ and $I_v(z)$ asymptote to

$$K_v(z) \approx \sqrt{\frac{\pi}{2z}}e^{-z}, \quad I_v(z) \approx \frac{e^z}{\sqrt{2\pi z}}. \tag{A.3a,b}$$

Thus, it follows that

$$\frac{K_{v+1}(z)}{K_v(z)} \approx \frac{K_{v+2}(z)}{K_v(z)} \approx \frac{I_{v+1}(z)}{I_v(z)} \approx \frac{I_{v+2}(z)}{I_v(z)} \approx 1. \tag{A.4a–d}$$

For $|z| \ll 1$, the Hankel functions asymptote to, when $v = 0$, [24]

$$H_0^{(2)}(z) \approx -H_0^{(1)}(z) \approx -i\frac{2}{\pi}\{\ln(z) + \gamma - \ln(2)\}, \tag{A.5a,b}$$

where $\gamma \approx 0.577\ldots$ is Euler's constant. When $\mathrm{Re}\{v\} > 0$,

$$H_v^{(2)}(z) \approx -H_v^{(1)}(z) \approx i\frac{\Gamma(v)}{\pi}\left(\frac{2}{z}\right)^v, \tag{A.6a,b}$$

where $\Gamma(v)$ is the gamma function with argument v, and

$$K_v(z) \approx \frac{\Gamma(v)}{2}\left(\frac{2}{z}\right)^v, \quad I_v(z) \approx \frac{1}{\Gamma(v+1)}\left(\frac{z}{2}\right)^v. \tag{A.7a,b}$$

References

[1] M.J. Lighthill, *Waves in Fluids*, Cambridge University Press, Cambridge, 1978.
[2] R.S. Langley, Wave evolution, reflection, and transmission along inhomogeneous waveguides, *Journal of Sound and Vibration* 227 (1999) 131–158.
[3] A.D. Pierce, *Acoustics: An Introduction to Its Physical Principles and Applications*, McGraw-Hill, New York, 1981.
[4] B.N. Nagarkar, R.D. Finch, Sinusoidal horns, *Journal of the Acoustical Society of America* 50 (1971) 23–31.
[5] N.W. McLachlan, *Bessel Functions for Engineers*, second ed., Oxford University Press, London, 1955.
[6] K.F. Graff, *Wave Motion in Elastic Solids*, Clarenden Press, Oxford, 1975.
[7] B.M. Kumar, R.I. Sujith, Exact solutions for the longitudinal vibration of non-uniform rods, *Journal of Sound and Vibration* 207 (1997) 721–729.
[8] E.T. Cranch, A.A. Adler, Bending vibrations of variable section beams, *Journal of Applied Mechanics* 23 (1956) 103–108.
[9] S. Abrate, Vibration of non-uniform rods and beams, *Journal of Sound and Vibration* 185 (1995) 703–716.
[10] E.D. Suppiger, N.J. Taleb, Free lateral vibration of beams of variable cross section, *Zeitschrift für Angewandte Mathematik und Physik (ZAMP)* 7 (1956) 501–520.
[11] H.D. Conway, E.C.H. Becker, J.F. Dubil, Vibration frequencies of tapered bars and circular plates, *Journal of Applied Mechanics* 31 (1964) 329–331.
[12] H.H. Mabie, C.B. Rogers, Transverse vibrations of tapered cantilever beams with end support, *Journal of the Acoustical Society of America* 44 (1968) 1739–1741.
[13] H.H. Mabie, C.B. Rogers, Transverse vibrations of double-tapered cantilever beams with end support and with end mass, *Journal of the Acoustical Society of America* 55 (1974) 986–991.
[14] R.P. Goel, Transverse vibrations of tapered beams, *Journal of Sound and Vibration* 47 (1976) 1–7.
[15] W.L. Craver, P. Jampala, Transverse vibrations of a linearly tapered cantilever beam with constraining springs, *Journal of Sound and Vibration* 166 (1993) 521–529.
[16] N.M. Auciello, G. Nole, Vibrations of a cantilever tapered beam with varying section properties and carrying a mass at the free end, *Journal of Sound and Vibration* 214 (1998) 105–119.
[17] J.R. Banerjee, F.W. Williams, Exact Euler–Bernoulli dynamic stiffness matrix for a range of tapered beams, *International Journal for Numerical Methods in Engineering* 21 (1985) 2289–2302.
[18] B.A.T. Petersson, E.J.M. Nijman, The one-dimensional bending wave counterpart to the acoustic horn and the semi-infinite wedge, *Journal of Sound and Vibration* 211 (1998) 95–121.
[19] V.V. Krylov, F.J.B.S. Tilman, Acoustic 'black holes' for flexural waves as effective vibration dampers, *Journal of Sound and Vibration* 274 (2004) 605–619.
[20] N.R. Harland, B.R. Mace, R.W. Jones, Wave propagation, reflection and transmission in tunable fluid-filled beams, *Journal of Sound and Vibration* 241 (2001) 735–754.
[21] J.F. Doyle, *Wave Propagation in Structures: Spectral Analysis using Fast Discrete Fourier Transforms*, Springer, New York, 1997.
[22] L. Cremer, M. Heckl, E.E. Ungar, *Structure-Borne Sound*, Springer, Berlin, 1973.
[23] S.-K. Lee, Wave Reflection, Transmission and Propagation in Structural Waveguides, PhD Thesis, University of Southampton, Institute of Sound and Vibration Research, 2006.
[24] M. Abramowitz, I.A. Stegun, *Handbook of Mathematical Functions with Formulas, Graphs, and Mathematical Tables*, Dover, New York, 1965.